JNeurosci
THE JOURNAL OF NEUROSCIENCE

Research Articles: Behavioral/Cognitive

Neural Representations of Faces are Tuned to Eye Movements

Lisa Stacchi, Meike Ramon, Junpeng Lao and Roberto Caldara

Eye and Brain Mapping Laboratory (iBMLab), Department of Psychology, University of Fribourg, Fribourg, Switzerland

https://doi.org/10.1523/JNEUROSCI.2968-18.2019

Received: 22 November 2018

Revised: 7 February 2019

Accepted: 5 March 2019

Published: 13 March 2019

Author contributions: L.S. and M.R. performed research; L.S. analyzed data; L.S. and M.R. wrote the first draft of the paper; L.S., M.R., J.L., and R.C. edited the paper; L.S. and M.R. wrote the paper; J.L. contributed unpublished reagents/analytic tools; R.C. designed research.

Conflict of Interest: The authors declare no competing financial interests.

This work was supported by the Swiss National Science Foundation (grant number IZLJZ1_171065/1) awarded to Roberto Caldara.

Corresponding author: Roberto Caldara, Department of Psychology, University of Fribourg, Faucigny 2, 1700 Fribourg, Switzerland, Email: roberto.caldara@unifr.ch, Tel: +41 (26) 300 76 36

Cite as: J. Neurosci 2019; 10.1523/JNEUROSCI.2968-18.2019

Neural Representations of Faces are Tuned to Eye Movements

Lisa Stacchi, Meike Ramon, Junpeng Lao, & Roberto Caldara*

Eye and Brain Mapping Laboratory (iBMLab), Department of Psychology, University of Fribourg, Fribourg, Switzerland

* Corresponding author:

Roberto Caldara

Department of Psychology

University of Fribourg

Faucigny 2

1700 Fribourg

Switzerland

Email: roberto.caldara@unifr.ch

Tel: +41 (26) 300 76 36

Running title: Neural Face Responses are Tuned to Eye Movements

Number of figures: 7

Number of tables: 3

Word count Abstract: 165

Word count Introduction: 648

Word count Discussion: 1068

Acknowledgements:

This work was supported by the Swiss National Science Foundation (grant number IZLJZ1_171065/1) awarded to Roberto Caldara.

ABSTRACT

Eye movements provide a functional signature of how human vision is achieved. Many recent studies have consistently reported robust idiosyncratic visual sampling strategies during face recognition. Whether these inter-individual differences are mirrored by idiosyncratic *neural* responses remains unknown. To this aim, we first tracked eye movements of male and female observers during face recognition. Additionally, for every observer we obtained an objective index of neural face discrimination through EEG that was recorded while they fixated different facial information. We found that facial features fixated longer during face recognition elicited stronger neural face discrimination responses across *all* observers when foveated. This relationship occurred independently of inter-individual differences in preferential facial information sampling (e.g., eye *vs.* mouth lookers), and started as early as the first fixation. Our data show that eye movements play a functional role during face processing by providing the neural system with the information that is diagnostic to a specific observer. The effective processing of identity involves idiosyncratic, rather than universal face representations.

SIGNIFICANT STATEMENT

When engaging in face recognition, observers deploy idiosyncratic fixation patterns in order to sample facial information. Whether these individual differences concur with idiosyncratic faces-sensitive neural responses remains unclear. To address this issue, we recorded observers' fixation patterns, as well as their neural face discrimination responses elicited during fixation of ten different locations on the face, corresponding to different types of facial information. Our data reveal a clear interplay between individuals' face-sensitive neural responses and their idiosyncratic eye movement patterns during identity processing, which emerges as early as the first fixation. Collectively, our findings favor the existence of idiosyncratic, rather than universal face representations.

INTRODUCTION

The visual system continuously processes perceptual inputs to adapt to the world by selectively moving the eyes towards task-relevant, i.e. diagnostic information. As a consequence, eye movements do not unfold randomly, and during face processing humans deploy specific gaze strategies. For many years, face recognition was considered to elicit a T-shaped fixation pattern encompassing the eye and mouth regions, which was universally shared across all observers (Yarbus, 1967; Henderson et al., 2005). However, over the last decade, a growing body of work has challenged this view by revealing cross-cultural (e.g., Blais et al., 2008; Miellet et al., 2013), idiosyncratic (Mehoudar et al., 2014), and within-observer (Miellet et al., 2011) differences during face recognition. For example, both Western and Eastern exhibit comparable face recognition proficiency while deploying respectively a T-shaped *vs.* more central fixation bias (for a review see Caldara, 2017). In addition, in line with early observations based on individual participants (Walker-Smith et al., 1977), recent studies demonstrate that observers deploy unique sampling strategies (Kanan et al., 2015; Arizpe et al., 2017), which are stable over time (Mehoudar et al., 2014), and relevant to behavioral performance (Peterson and Eckstein, 2013). Specifically, individuals' sampling strategies deviate considerably from the well-established T-shaped pattern, which is merely the result of the group averaging of idiosyncratic visual sampling strategies of individual Western observers (Mehoudar et al., 2014).

Despite the growing literature on the existence of idiosyncratic sampling strategies, their functional role and underlying neural mechanisms remain poorly understood. Some studies have investigated the impact of the fixated facial information input on neural responses, by recording the electroencephalographic (EEG) signals while observers fixated different facial information (i.e., viewing positions; VPs). This body of work has focused on the N170 face-sensitive ERP (Event Related Potential) component (Bentin et al., 1996), and has demonstrated

that VPs differentially modulate the N170. The finding of the eye region eliciting larger amplitudes (de Lissa et al., 2014, Itier et al., 2006; Nemrodov et al., 2014; Rousselet et al., 2014) has been interpreted in terms of a universal *neural* preference toward this facial information. However, these studies have mainly involved grand-average analyses, and did not control for *individual* fixation preferences. Consequently, it remains unclear whether idiosyncratic fixation biases concur with idiosyncratic neural responses.

A paradigm that has been increasingly used to examine different aspects of face processing, including e.g. face categorization, identity or facial expression discrimination (Liu-Shuang et al., 2014; Norcia et al., 2015; Rossion et al., 2015; Dzhelyova et al., 2016) involves fast-periodic visual stimulation (FPVS). Such FPVS paradigms involve stimulation with a series of stimuli that periodically differ with respect to a given dimension. Neural synchronization to the frequency of changes provides an implicit measure of the process of interest. Compared to traditional ERPs, the FPVS response is less susceptible to noise artefacts, and its remarkably high signal-to-noise ratio increases the likelihood of detecting subtle differences between experimental manipulations (Norcia et al., 2015). Such signal properties make the FPVS paradigm paired with EEG recordings ideal to investigate the relationship between VP-dependency of neural responses and idiosyncratic visual sampling strategies.

In the present study, we extracted observers' fixation patterns exhibited during an old/new face recognition task (Blais et al., 2008). Additionally, we recorded their neural face discrimination responses using a FPVS paradigm, in which same identity faces were presented at a constant frequency rate with periodically intervening oddball identities, while observers fixated one of ten VPs. We then applied a robust data-driven statistical approach to relate the idiosyncratic sampling strategies to the electrophysiological responses across all electrodes independently. As early as the first fixation, we find a strong positive relationship between

idiosyncratic sampling strategies and neural face discrimination responses recorded across different VPs, which can be observed across all observers. In particular, independently of the sampling strategy, the longer a VP was fixated under natural viewing conditions, the stronger the neural face discrimination response during its enforced fixation.

METHODS

Participants

The sample size opted for was motivated by studies using the same FPVS paradigm to index neural face discrimination that were published up to data acquisition (Dzhelyova and Rossion, 2014a, 2014b, Liu-Shuang et al., 2014, 2016; sample size range: 8-12). In Dzhelyova and Rossion's (2014b) study using a within subject design, the observed minimal effect size resulting from a repeated ANOVA was .2 (partial-eta). As the effect size estimation is often overly optimistic in the literature, we planned our experiment based on an effect size of .1 and an estimated sample size of 15 participant which results in a power of .95 to detect an effect. Based on prior experience and the requirement of high-quality data from independent methods, we chose to test a total number of 20 participants. Our cohort comprised 20 Western Caucasian observers (11 females, two left-handed, mean age: 25±3 years) with normal or corrected-to-normal vision and no history of psychiatric or neurological disorders. Three observers were excluded due to poor quality of the eye movement data. All participants provided written informed consent and received financial compensation for participation; all procedures were approved by the local ethics committee. Finally, all observers performed the eye-tracking and the EEG experiment during the same testing session and systematically in this order. It is worth noting, that the stimuli used across those sessions are different and cannot account for an order effect. In addition, none of the observers were aware of their fixation biases.

Procedures

Eye-tracking

Experimental design

Stimuli consisted of 56 Western Caucasian (i.e. WC) and 56 East Asian (i.e. EA) identities respectively obtained from the KDEF (Lundqvist et al., 1998) and the AFID (Bang et al., 2001). Faces were presented at a viewing distance of 75 cm and subtended 12.56° (height from chin to hairline) x 9.72° (width) of visual angle on a VIEWPIxx/3D monitor (1920 x 1080 pixel resolution, 120 Hz refresh rate).

Observers completed two learning and recognition blocks per stimulus race. In each block, observers were instructed to learn 14 face identities (7 females) randomly displaying either neutral, happy or disgust expressions. After a 30 second pause, a series of 28 faces (14 old faces) were presented and observers were instructed to indicate as quickly and as accurately as possible whether each face was familiar or not by key-press. To prevent image matching strategies, learned identities displayed different facial expression in the recognition blocks. Each trial involved presentation of a central fixation dot (which also served as an automatic drift correction), followed by a face presented pseudorandomly in one of four quadrants of the computer screen, to avoid potential anticipatory fixation strategies. During the learning phase, stimuli were presented for five seconds; during the recognition phase presentation was terminated upon participants' responses. Eye movements were recorded during both the learning and recognition phases.

Data acquisition and processing

The oculomotor behavior was recorded for each participant using an EyeLink 1000 Desktop Mount with a temporal resolution of 1000 Hz. The raw data are available in the public domain

(Stacchi et al., 2018). Data were registered by using the Psychophysics (Brainard, 1997) and the EyeLink (Cornelissen et al., 2002) Toolbox running in a MatlabR2013b environment. Calibrations and validations were performed at the beginning of the experiment using a nine-point fixation procedure. Additionally, before each trial a fixation cross appeared in the center of the screen and participants were instructed to fixate on it until a new stimulus appeared to ensure that eye movements were correctly tracked. A new calibration was performed at this stage if the eye drift exceeded 1° of visual angle.

After removing eye blinks and saccades using the algorithm developed by Nystrom et al. (Nyström and Holmqvist, 2010), observers' eye movement data from the Old-New task were processed to create individual fixation maps, independently for learning and recognition phase. For both phases we removed noisy trials suffering from loss of data and/or precision and for the recognition session we only considered trials where subjects provided a correct response. Previous studies have shown that with this paradigm there are no differences in the sampling strategies used to sample WC or EA faces (Blais et al., 2008; Caldara, 2017). Therefore, in order to increase the signal-to-noise ratio, fixation maps were extracted independently of the stimulus race. After pre-processing the eye movement data, fixation maps were computed independently for each subject based on 54 and 60 trials for the learning and recognition phase respectively. These were the minimum number of trials available for all subjects. Individuals' fixation intensities (based on the cumulative fixation duration) were derived using these fixation maps and pre-defined circular regions of interest (ROIs; see Fig. 1). The ROIs covered 1.8° of visual angle and were centered on the ten viewing positions fixated during the FPVS experiment.

EEG

Experimental design

We used full-front, color images of 50 identities (25 female) from the same set described previously (Liu-Shuang et al., 2014). All faces conveyed a neutral expression, were cropped to exclude external facial features, and were presented against a grey background. Each original stimulus subtended 11.02° (height) x 8.81° (width) of visual angle at a viewing distance of 70 cm.

Face-stimuli were displayed through the fast periodic visual stimulation (i.e., FPVS) paradigm at a constant frequency rate of 6 Hz. Each trial lasted 62s and consisted in presenting a series of same-identity faces (i.e., base), with intervening oddball identities every 7th base, hence at a frequency of 0.857 Hz (Fig. 2A-C). The experiment comprised a total of 20 trials: ten conditions (the viewing positions participants were required to fixate on; Fig. 2B-C), with two trials per condition (trials differed with respect to the gender of the face stimuli). To prevent eye-movements, participants were instructed to maintain fixation on a central cross. The position of face stimuli was manipulated to vary, across trials, the fixated viewing position, hence the facial information. Faces were presented through sinusoidal contrast modulation (see Fig. 2A). Additionally, two seconds of gradual fade in and fade out were added at the beginning and end of each trial. To maintain subjects' attention, the fixation cross briefly (200ms) changed color (red to blue) randomly between seven and eight times within each trial; participants were instructed to report the color change by button press. Subjects were also monitored through a camera placed in front of them communicating the experimenter computer. No additional eye-tracking was performed during EEG acquisition, as these measures were considered as sufficient for the intended purposes. Finally, to avoid pixel-wise overlap, stimulus size varied randomly from 80% to 120% of the original size (visual angle

ranged from 8.82-13.22° (height) to 7.05-10.57° (width)).

Data acquisition and processing

Electrophysiological responses were recorded with Biosemi Active-Two amplifier system (Biosemi, Amsterdam, Netherlands) with 128 Ag/AgCl active electrodes and a sampling rate of 1024Hz. Electrodes were relabeled according to the more conventional 10-20 system notation following the guidelines by Liu-Shuang et al. (2015). Additional electrodes placed at the outer canthi and below both eyes registered eye movements and blinks; the magnitude of the offset of all electrodes was reduced and maintained below ±25mV. The recorded EEG was analyzed using Letswave 5 (https://github.com/NOCIONS/Letswave5); (Mouraux and Iannetti, 2008)). The raw data are available in the public domain (Stacchi et al., 2018). Preprocessing consisted in high- and low-pass filtering the signal (with a 0.1Hz and 100Hz Butterworth band-pass filter (4^{th} order)). Data were subsequently downsampled to 256Hz and segmented according to condition resulting in 20 66-second epochs, which included two seconds before and after stimulation. Independent component analysis was performed on each participant's data to remove contamination due to eye-movements and blinks.

Noisy electrodes were interpolated using the three nearest spatially neighboring channels; this process was applied to no more than 5% of all scalp electrodes. Segments were then re-referenced to a common average reference and cropped to an integer number of oddball cycles, excluding two seconds after stimulus onset and two seconds before stimulus offset (~58-second epochs; 14932 bins). Epochs were then averaged separately for each subject per condition.

Frequency domain

Fast Fourier Transform (FFT) was applied to the averaged segments and amplitude was

extracted. The data were baseline corrected by subtracting from each frequency's amplitude the average of its surrounding 20 bins excluding the two neighboring ones. Finally, for each subject and condition, the summed baseline-corrected amplitude of the oddball frequency and its significant harmonics provided the index of neural face discrimination. Following previous procedures (Dzhelyova et al., 2016), harmonics were considered significant until the mean z-score across all conditions was no longer above 1.64 ($p<.05$). Based on this criterion we considered the first 11 harmonics excluding the 7th harmonic, which is confounded with the base stimulation frequency rate.

Statistical analyses

Using the iMAP4 toolbox (Lao et al., 2017) we computed a linear regression to explore the relationship between the fixation bias (the z-scored fixation duration) displayed during the recognition phase and neural face discrimination (i.e., the FPVS response amplitude). To this aim we performed a linear mixed-effects model with random effect for intercept and *Fixation duration* grouped by subject. To avoid a-priori assumptions regarding topography of the effect, we regressed the two variables at all scalp electrodes independently and results were Bonferroni-corrected.

$$FPVS\_amplitude \sim 1 + Fixation\_duration + (1 + Fixation\_duration \mid Subjects) \quad (1)$$

This computation will determine whether, VP-dependent fixation duration are associated with the amplitude of the neural face discrimination response elicited by each VP. Importantly, because the analysis takes into consideration idiosyncrasies, there is no a priori expectation on how VPs are ranked. We opted for this approach in light of individual differences in fixation patterns reported previously (Mehoudar et al., 2014; Arizpe et al., 2016; Kanan et al., 2015), and similar idiosyncrasies assumed to exist for neural face discrimination responses across VPs.

213 Therefore, the model used here allows each subject to have his/her specific VP-pattern and a
214 relationship emerges if the fixation pattern is predictive of the neural response pattern of the
215 same subject. Finally, as the current work does only focus on individual subjects, we did not
216 perform any analysis involving average fixation maps and average EEG responses.

217 To determine whether fixation maps would show a stronger correlation with EEG responses of
218 the same subject, we randomly sampled the fixation maps of our subjects in order to correlate
219 eye movement from one observer with EEG response of another observer. On these new data
220 we performed the same regression described above. This process was repeated a thousand
221 times, and within each iteration we summed the significant F-values ($p<0.5/128$). We then
222 ranked the one thousand summed significant F-values and selected the 95th percentile as the
223 threshold to assess statistical significance. Only if the summed significant F-values from the
224 original analysis were above this simulated threshold, results were retained as being significant.

225 Additionally, although the main focus of this work was to isolate the relationship between eye
226 movements during correct recognition of faces and neural face discrimination responses, in
227 order to provide a comprehensive view of our data we also investigated whether such
228 relationship would occur when considering fixation biases based on the (i) first or (ii) second
229 face fixations in each trial. Moreover, we also performed the same analysis by considering the
230 eye movements of the learning phase. We thus investigated the potential existence of such
231 relationship between eye movements and neural face discrimination for (i) all fixations, (ii) the
232 first or (iii) the second only for the learning and recognition phases.

RESULTS

Behavior

As expected, subjects' recognition performance in the Old-New task, as indexed by d', was significantly better for Western Caucasian (M=1.62, SD=.64) than East Asian faces (M=0.97, SD=.60), t(16)=5.72, $p<.01$. Subjects' performance was nearly at ceiling for the FPVS orthogonal task (M=.91, SD=.18). Note that a color change was considered as detected if observers reported it within 700ms from its onset. Due to technical issues, one subject's behavioral responses were not recorded.

Eye-movements and FPVS response

Description of fixation and neural biases at the group and individual level

Table 1 summarizes the number of fixations and the similarity between fixation maps during learning and recognition sessions (indexed by the cosine distance, with a distance of zero indicating identical fixation maps). The average fixation map (computed for descriptive purposes and shown in Fig. 3A) demonstrates that, *as a group,* observers preferentially sampled facial information encompassing the eyes, nasion, nose and mouth. However, because the focus of this work was to investigate the relationship between fixation patterns and neural responses at the individual level, group data were not subject to any further analysis.

At the individual level, the majority of individual observers' fixation maps did not *perfectly* conform to the grand average fixation pattern (Fig. 3A-B; Fig. 4), clearly demonstrating the existence of idiosyncratic visual sampling strategies. Mirroring these results, the grand average neural face discrimination response amplitudes varied as a function of VPs,

with the greatest amplitudes for the central position (Fig. 3C). However, the neural responses amplitudes also markedly differed across individuals (Fig. 3D; Fig. 4).

Regression analysis: Assessing the relationship between fixation and neural biases

The data-driven regression between individuals' fixation durations and FPVS responses across VPs computed independently on all electrodes revealed a positive relationship at right occipito-temporal and central-parietal clusters (see Fig. 5A).

The occipito-temporal cluster includes 12 significant electrodes with the strongest effect at P10 ($F(1,169)=32.91$, ß=.27 [.17 .36], p=4.40e-08) and the smallest at P9 ($F(1,169)=13.26$ ß=.20 [.09 .31], p=3.61e-04) (Table 2). Despite inter-individual variations in the neural face discrimination response amplitude and fixation durations, we observed a positive relationship for *all* observers (Fig. 5B-C).

An effect was also found on the central-parietal cluster comprising 13 electrodes, with C1 showing the strongest effect ($F(1,169)=33.05$ ß=.14 [.09 .19], p=4.14e-08) and FCz exhibiting the smallest effect ($F(1,169)=15.41$ ß=.12 [.06 .18], p=1.26e-4) (Fig. 5A; Table 2).

Finally, in order to determine whether fixation maps would correlate better with EEG responses of the same subject, we run simulations of the same analyses when EEG responses were correlated with fixation maps of different observers. In each iteration we summed the significant F-value and the 95th percentile of this distribution constituted our simulated threshold (see Data analyses). The sum of significant F-values (670.89) obtained using the original data exceeded the simulated threshold determined (536.32), and was therefore significant (Table 2). Significant results were also obtained for analyses carried out on the *first* (summed F-values = 474.07, simulated threshold = 345.67) and the *second* fixation (summed F-values = 500.79, simulated threshold = 310.82) (Fig. 6B; Table 2). The results of the same

277 analyses performed on data acquired during the learning session were significant only for the
278 first fixation (summed F-values = 447.33, simulated threshold = 315.06) (Fig. 6A; Table 3).

279 *Can **specific** fixation biases account for the observed relationship?*

280 To explore whether subjects exhibiting a particular fixation bias during recognition
281 (e.g., for the eyes) would show a stronger relationship between fixation and neural biases, we
282 first ranked observers' fixation maps based on the magnitude of their individual relationship.
283 As shown in Figure 7A, subjects showing similar fixation patterns could exhibit relationships
284 of slightly different magnitude (e.g., nasion: S04 and S05), while observers exhibiting different
285 fixation maps could rank closely in terms of relationship strengths (e.g., S11 and S16).
286 Additionally, we computed the distance of each observer's fixation map from the average
287 fixation pattern. In this case, each map is treated as a vector and the measure of interest is the
288 cosine distance between each observers' map and the average one (a distance of zero indicates
289 identical fixation maps). This produces a value ranging between 0 and 1 for each subject. The
290 higher the distance the more dissimilar that given subject's pattern is from the average. Finally,
291 we performed a Spearman correlation between this distance and the strength of the relationship
292 between fixation and neural bias, which resulted to be non-significant ($r=-.31$, $p=.22$) (Fig. 7B).

293 **DISCUSSION**

294 This study investigated the relationship between *idiosyncratic* visual sampling strategies for
295 faces and the magnitude of neural face discrimination responses during fixation on different
296 facial locations. Our data show that visual information sampling is distinct across observers,
297 and these differences are positively correlated with *idiosyncratic* neural responses
298 predominantly at occipito-temporal electrodes. Specifically, the Viewing Positions (VPs) that
299 elicited stronger neural face discrimination responses coincided with the VPs that were more

fixated under free-viewing conditions. Altogether, our data show that face processing involves idiosyncratic coupling of *distinct* information sampling strategies and *unique* neural responses to the preferentially sampled facial information.

For many years, the accepted notion in vision research was that face processing elicits a unique and universal cascade of perceptual and cognitive events to process facial identity, with particular importance ascribed to information conveyed by the eye region. For instance, eye movement studies have revealed a bias towards sampling of the eye region (Blais et al., 2008), the diagnosticity of which has been further documented by psychophysical approaches (e.g., Bubbles) (Gosselin and Schyns, 2001). Electrophysiological studies have also reported increased N170 magnitude during fixation on the eyes, compared to other information (de Lissa et al., 2014; Nemrodov et al., 2014). Collectively, these independent findings were taken to support the existence of a fixation and neural preference for the eye-region that is shared across *all* observers.

However, this idea has recently been challenged. For example, findings from eye movement studies emphasize idiosyncrasies in sampling preferences that are highly distinct from the group-average T-shaped pattern (Mehoudar et al., 2014; Arizpe et al., 2017), or by the existence of cultural differences (Blais et al., 2008; Caldara, 2017). These individual differences are not systematically associated with performance, as "mouth lookers" (i.e., observers showing preferential fixation on the mouth) could perform similarly to "eyes lookers". Equally, two "eyes lookers" could exhibit very different performance (Peterson and Eckstein, 2013). Nonetheless, each observer's adopted sampling strategy is optimal in the sense that performance is maximal when fixation is enforced on preferably sampled information, and decreases during fixation of other information (Peterson and Eckstein, 2013). These results

suggest that individual differences do not reflect random inter-subject variation, but rather subtend functional idiosyncrasies in face processing.

Our results replicate and extend these previous findings, by showing that idiosyncratic visual sampling strategies strikingly mirror individuals' patterns of neural face discrimination responses across VPs. Specifically, the facial regions preferentially sampled during natural viewing were those eliciting stronger neural face discrimination responses when fixated. This pattern was present in all observers, with even some of them showing a perfect match between the most fixated facial feature and the one eliciting the strongest neural response at the electrode showing the strongest statistical relationship.

Interestingly, such relationship emerged also when fixation bias was computed only based on the first or the second fixation. This observation suggests that from very early information intake fixations are directed towards observer-specific preferred face information. Moreover, it also indicates that idiosyncratic fixation strategies emerge as early as the first fixation on faces.

When considering single fixations performed during face learning, a significant relationship emerged only on the first one. The reduced sensitivity of the learning phase compared to the recognition phase, might be due to the imposed time duration (i.e., 5 seconds) to process faces during this part of the experiment. This long time period introduces an inherent variability in information sampling. In the recognition session, however, observers are required to recognize faces as quickly and as accurately as possible, eliciting a restricted number of diagnostic fixations (Table 1) during a short period of time (i.e., M = 1457.3, SD = 421.3). However, it is worth noting that overall observers deployed similar fixations across both sessions (Table 1), a result that reinforces the idea of a reliable occurrence of idiosyncratic eye

346 movement strategies over (a long period of) time (Mehoudar et al., 2014) for the face
347 recognition task.

348 The effect we find could be partially related to an overall preference toward facial
349 features, such as the eyes and mouth or the center of the face (i.e., T-shaped pattern). However,
350 significantly weaker effects are observed when correlating fixation maps and neural response
351 derived from different individuals. These observations clearly demonstrate the existence of a
352 tight coupling between idiosyncratic fixation biases and neural responses, instead of a general
353 tuning for facial features per se.

354 The strong and striking relationship between information sampling and neural
355 idiosyncrasies suggests a functionally relevant process. Eye movements feed the neural face
356 system with the diagnostic information in order to optimize information processing. The eyes
357 constantly move to center elements of interest in the fovea, where visual acuity is greatest. This
358 critical functional role, coupled with the relationship reported here between idiosyncratic
359 sampling strategies and the neural face discrimination response pattern thus leads to two main
360 considerations. First, our data show that face identity processing involves a fine-tuned interplay
361 between oculomotor mechanisms and face-sensitive neural network. Second, the diagnosticity
362 associated with different facial information varies across observers. For a long time,
363 researchers have debated on the nature of face representations, mainly opposing the idea of
364 faces being represented as indivisible wholes (holistic or configural), as opposed to a collection
365 of multiple, distinctively perceivable features (featural). This ongoing debate cannot be settled
366 based on our finding of visual and neural idiosyncrasies. These idiosyncrasies do, however,
367 refute the concept of a *single* face representation format shared across observers.

368 Our observations raise further important methodological and theoretical questions. The
369 first concerns the traditional approach of standardizing the visual input to allow comparability

370 across observers. The idiosyncratic differences in facial location tuning call into question the
371 appropriateness of using a single visual stimulation location. Specifically, the conventional
372 central presentation used in the majority of face processing studies might inherently create a
373 perceptual bias that favors some but not all observers, which exhibit differential neural
374 responses for this fixation location (and others). Additional open questions concern for instance
375 (a) the extent to which the relationship between the visual sampling strategies and neural
376 response patterns is *task*- and *category*-specific, and (b) the direction of this relationship.
377 Future studies are required to accurately determine the neural structures underlying the
378 observed relationship (for example, by means of fMRI). Finally, our approach may offer a
379 promising novel route in clinical settings, if disorders comprising face processing impairments
380 (i.e., prosopagnosia, autism, schizophrenia, etc.) involved an abnormal relationship between
381 fixation patterns and neural responses to faces.

382 **REFERENCES**

383 Arizpe J, Walsh V, Yovel G, Baker CI (2017) The categories, frequencies, and stability of
384 idiosyncratic eye-movement patterns to faces. Vision Res 141:191–203
385 https://linkinghub.elsevier.com/retrieve/pii/S0042698916301845 .
386 Bang S, Kim D, Choi S (2001) Asian Face Image Database. In: Lab IM. Postech, Korea.
387 Bentin S, Allison T, Puce A, Perez E, McCarthy G (1996) Electrophysiological Studies of Face
388 Perception in Humans. J Cogn Neurosci 8:551–565
389 http://www.mitpressjournals.org/doi/10.1162/jocn.1996.8.6.551 .
390 Blais C, Jack RE, Scheepers C, Fiset D, Caldara R (2008) Culture Shapes How We Look at
391 Faces Holcombe AO, ed. PLoS One 3:e3022
392 http://dx.plos.org/10.1371/journal.pone.0003022 .
393 Brainard DH (1997) The Psychophysics Toolbox. Spat Vis:433–436.
394 Caldara R (2017) Culture Reveals a Flexible System for Face Processing. Curr Dir Psychol Sci
395 26:249–255 http://journals.sagepub.com/doi/10.1177/0963721417710036 .
396 Cornelissen FW, Peters EM, Palmer J (2002) The Eyelink Toolbox: Eye tracking with
397 MATLAB and the Psychophysics Toolbox. Behav Res Methods, Instruments, Comput.
398 de Lissa P, McArthur G, Hawelka S, Palermo R, Mahajan Y, Hutzler F (2014) Fixation location
399 on upright and inverted faces modulates the N170. Neuropsychologia 57:1–11
400 http://linkinghub.elsevier.com/retrieve/pii/S002839321400058X .
401 Dzhelyova M, Jacques C, Rossion B (2016) At a Single Glance: Fast Periodic Visual
402 Stimulation Uncovers the Spatio-Temporal Dynamics of Brief Facial Expression Changes
403 in the Human Brain. Cereb Cortex 27:4106–4123
404 http://cercor.oxfordjournals.org/cgi/doi/10.1093/cercor/bhw223 .
405 Dzhelyova M, Rossion B (2014a) The effect of parametric stimulus size variation on individual
406 face discrimination indexed by fast periodic visual stimulation. BMC Neurosci 15:87

http://bmcneurosci.biomedcentral.com/articles/10.1186/1471-2202-15-87.

Dzhelyova M, Rossion B (2014b) Supra-additive contribution of shape and surface information to individual face discrimination as revealed by fast periodic visual stimulation. J Vis 14:15–15.

Gosselin F, Schyns PG (2001) Bubbles: a technique to reveal the use of information in recognition tasks. Vision Res 41:2261–2271 http://linkinghub.elsevier.com/retrieve/pii/S0042698901000979.

Henderson JM, Williams CC, Falk RJ (2005) Eye movements are functional during face learning. Mem Cognit 33:98–106.

Itier RJ, Latinus M, Taylor MJ (2006) Face, eye and object early processing: What is the face specificity? Neuroimage 29:667–676 http://linkinghub.elsevier.com/retrieve/pii/S1053811905005653 .

Kanan C, Bseiso DNF, Ray NA, Hsiao JH, Cottrell GW (2015) Humans have idiosyncratic and task-specific scanpaths for judging faces. Vision Res 108:67–76 http://linkinghub.elsevier.com/retrieve/pii/S0042698915000292.

Lao J, Miellet S, Pernet C, Sokhn N, Caldara R (2017) iMap4: An open source toolbox for the statistical fixation mapping of eye movement data with linear mixed modeling. Behav Res Methods 49:559–575.

Liu-Shuang J, Norcia AM, Rossion B (2014) An objective index of individual face discrimination in the right occipito-temporal cortex by means of fast periodic oddball stimulation. Neuropsychologia 52:57–72 http://linkinghub.elsevier.com/retrieve/pii/S0028393213003801 .

Liu-Shuang J, Torfs K, Rossion B (2016) An objective electrophysiological marker of face individualisation impairment in acquired prosopagnosia with fast periodic visual stimulation. Neuropsychologia 83:100–113

http://linkinghub.elsevier.com/retrieve/pii/S0028393215301391.

Lundqvist D, Flykt A, Öhman A (1998) The Karolinska directed emotional faces. Stockholm, Sweden: Karolinska Institute.

Mehoudar E, Arizpe J, Baker CI, Yovel G (2014) Faces in the eye of the beholder: Unique and stable eye scanning patterns of individual observers. J Vis 14:6 http://jov.arvojournals.org/article.aspx?doi=10.1167/14.7.6 .

Miellet S, Caldara R, Schyns PG (2011) Local Jekyll and Global Hyde. Psychol Sci 22:1518–1526 http://journals.sagepub.com/doi/10.1177/0956797611424290 .

Miellet S, Vizioli L, He L, Zhou X, Caldara R (2013) Mapping Face Recognition Information Use across Cultures. Front Psychol 4:34 http://journal.frontiersin.org/article/10.3389/fpsyg.2013.00034/abstract .

Mouraux A, Iannetti GD (2008) Across-trial averaging of event-related EEG responses and beyond. Magn Reson Imaging 26:1041–1054 http://www.ncbi.nlm.nih.gov/pubmed/18479877 .

Nemrodov D, Anderson T, Preston FF, Itier RJ (2014) Early sensitivity for eyes within faces: A new neuronal account of holistic and featural processing. Neuroimage 97:81–94 http://linkinghub.elsevier.com/retrieve/pii/S1053811914003115 .

Norcia AM, Appelbaum LG, Ales JM, Cottereau BR, Rossion B (2015) The steady-state visual evoked potential in vision research: A review. J Vis 15:4 http://jov.arvojournals.org/article.aspx?doi=10.1167/15.6.4.

Nyström M, Holmqvist K (2010) An adaptive algorithm for fixation, saccade, and glissade detection in eyetracking data. Behav Res Methods 42:188–204 http://www.springerlink.com/index/10.3758/BRM.42.1.188 .

Peterson MF, Eckstein MP (2013) Individual Differences in Eye Movements During Face Identification Reflect Observer-Specific Optimal Points of Fixation. Psychol Sci 24:1216–

1225 http://journals.sagepub.com/doi/10.1177/0956797612471684 .

Rossion B, Torfs K, Jacques C, Liu-Shuang J (2015) Fast periodic presentation of natural images reveals a robust face-selective electrophysiological response in the human brain. J Vis 15:18–18 http://jov.arvojournals.org/Article.aspx?doi=10.1167/15.1.18 .

Rousselet GA, Ince RAA, van Rijsbergen NJ, Schyns PG (2014) Eye coding mechanisms in early human face event-related potentials. J Vis 14:7–7 http://jov.arvojournals.org/Article.aspx?doi=10.1167/14.13.7 .

Walker-Smith GJ, Gale AG, Findlay JM (1977) Eye Movement Strategies Involved in Face Perception. Perception 6:313–326 http://journals.sagepub.com/doi/10.1068/p060313.

Yarbus AL (1967) Eye Movements During Perception of Complex Objects. In: Eye Movements and Vision, pp 171–211. Boston, MA: Springer US.

FIGURES

Fig. 1. Illustration of the regions of interest (ROI) surrounding the 10 viewing positions (VPs). Observers' fixation maps were overlaid onto a ROI mask to compute the fixation intensity per ROI. The ROI were covering 1.8° of visual angle and were centered on 9 equidistant viewing positions (red circles) and on an additional VP corresponding to the center of the stimulus (black circle).

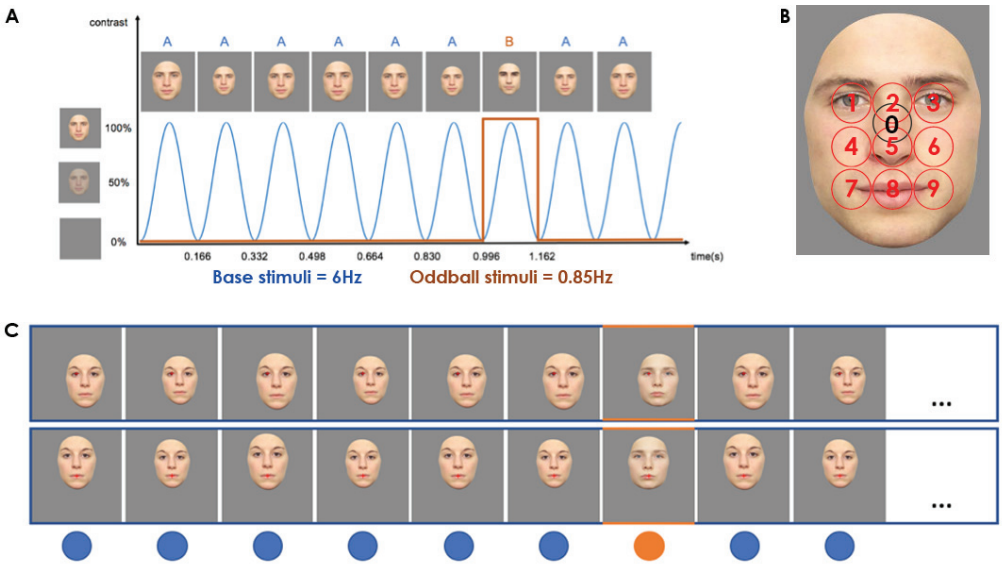

Fig. 2. FPVS paradigm and viewing positions. (A) Faces were presented at a frequency rate of 6Hz through sinusoidal contrast modulation. Base stimuli consisted of images of the same facial identity; interleaved oddball stimuli conveying different identities were presented every 7th base stimulus. (B) Illustration of the 10 viewing positions (VPs) fixated by participants. (C) Examples of two trials displaying fixation on the left eye (VP1, top row), or mouth (VP8, bottom row).

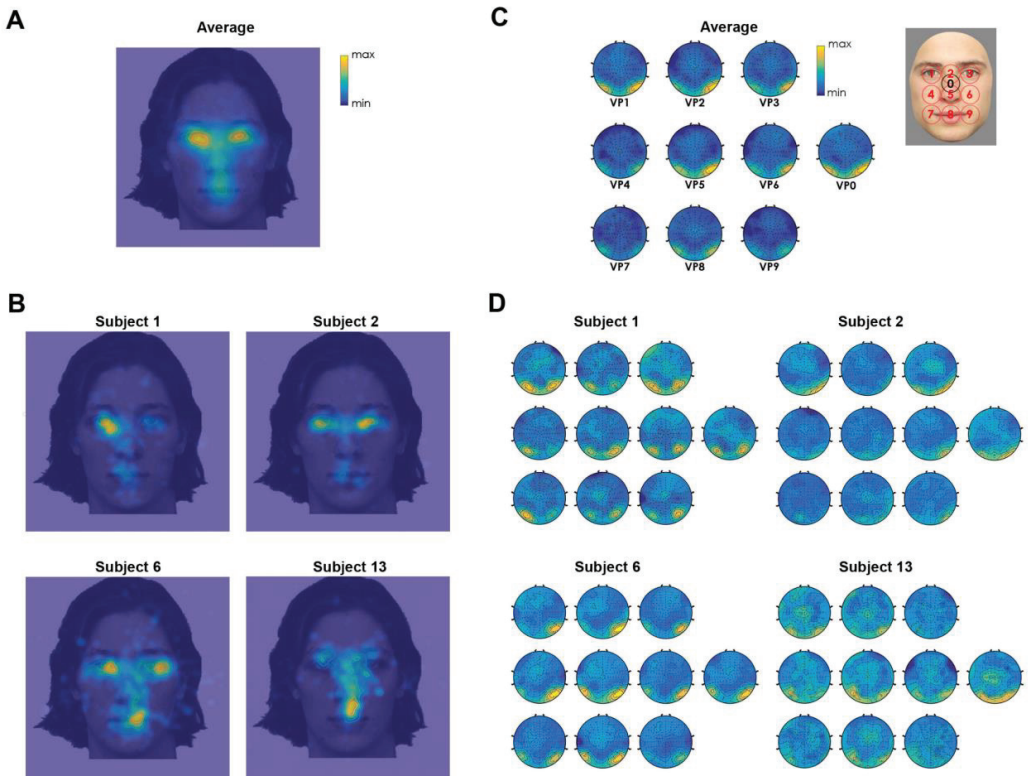

Fig. 3. Fixation maps and oddball responses. A and C show the grand-average fixation map and FPVS responses respectively, while B and D show the two measures for the same subjects. For illustration, only four subjects are reported.

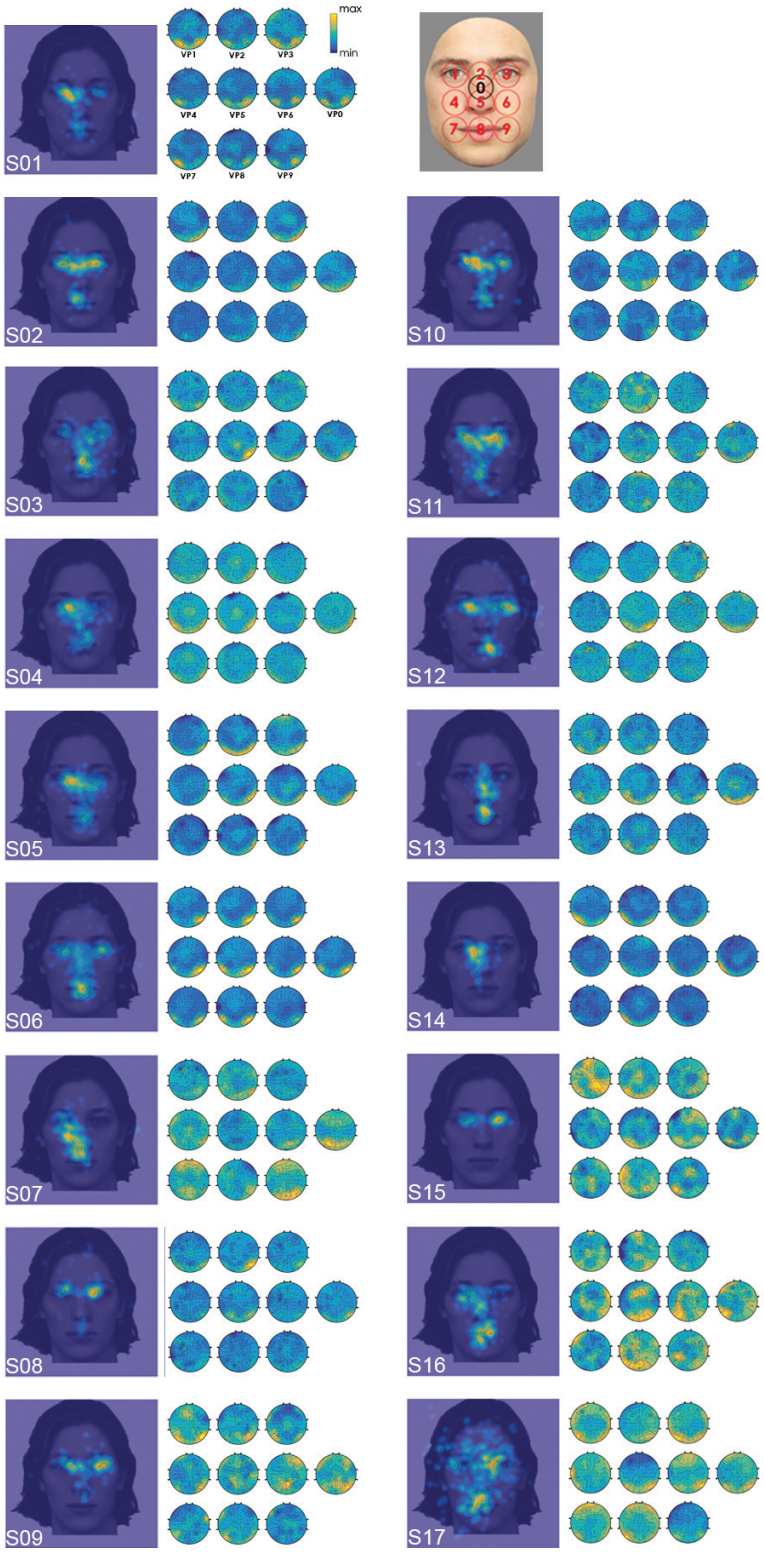

Fig. 4. Fixation maps for the recognition session and neural face discrimination responses of all subject

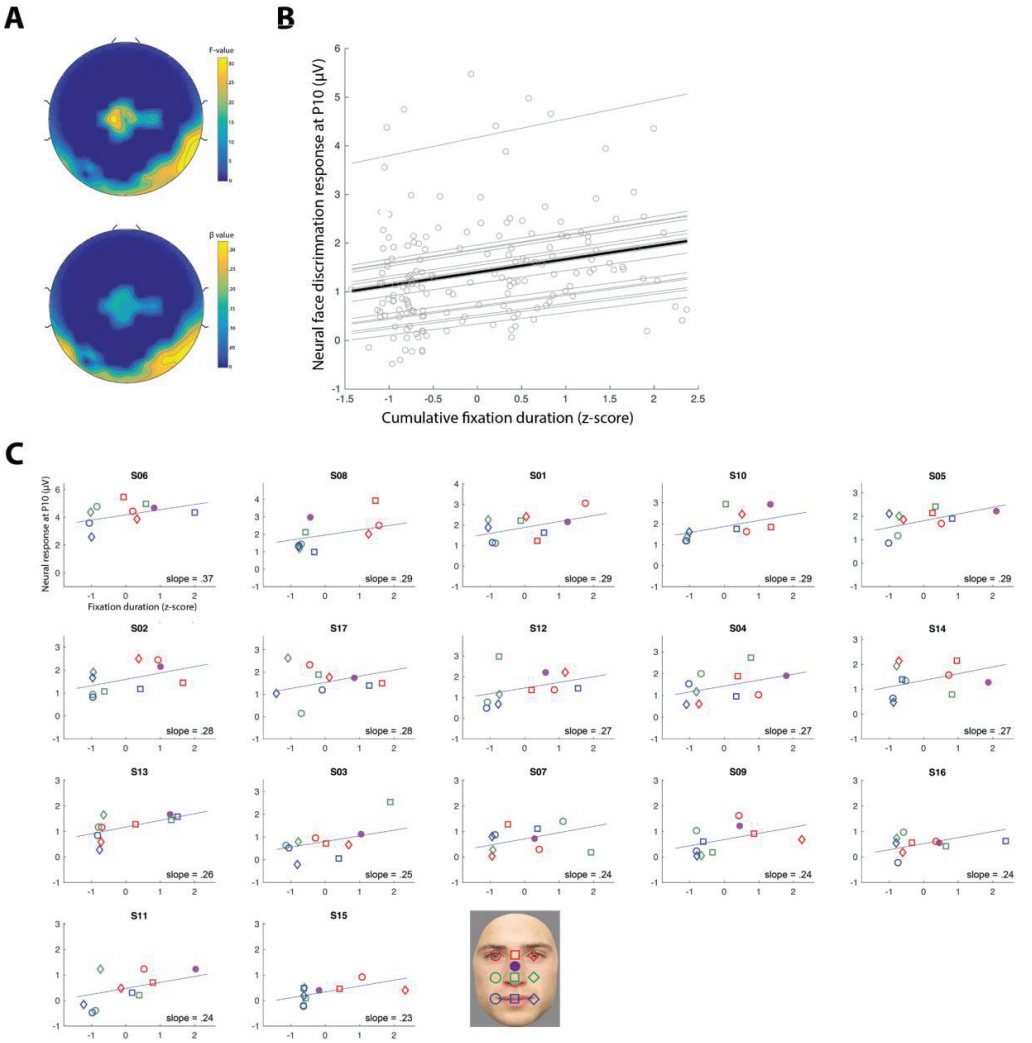

Fig 5. The relationship between fixation duration and neural face discrimination responses across VPs observed across all subjects considered individually. (A) Regression F-values (left) and beta maps (right) are shown only for electrodes exhibiting a significant effect ($p < 3.91e-04$) (B) Scatterplot illustrates individual subjects' (light grey lines) as wells as the group (black line) effect at electrode P10. (C) Zoom in into B. Each subject is plotted alone with their individual correlation (blue line). VPs are color- and shape-coded as indicated in the legend. The subjects are ordered as a function of their relationship magnitude (slope). Although observers exhibited idiosyncratic VP-dependent fixation durations (see also individuals' fixation maps in the following Fig. 7), all showed a positive relationship, with facial features fixated longer (i.e., VPs) eliciting stronger neural responses. Note that here the neural face discrimination response magnitude is displayed at the occipito-temporal electrode showing the largest effect (i.e., P10).

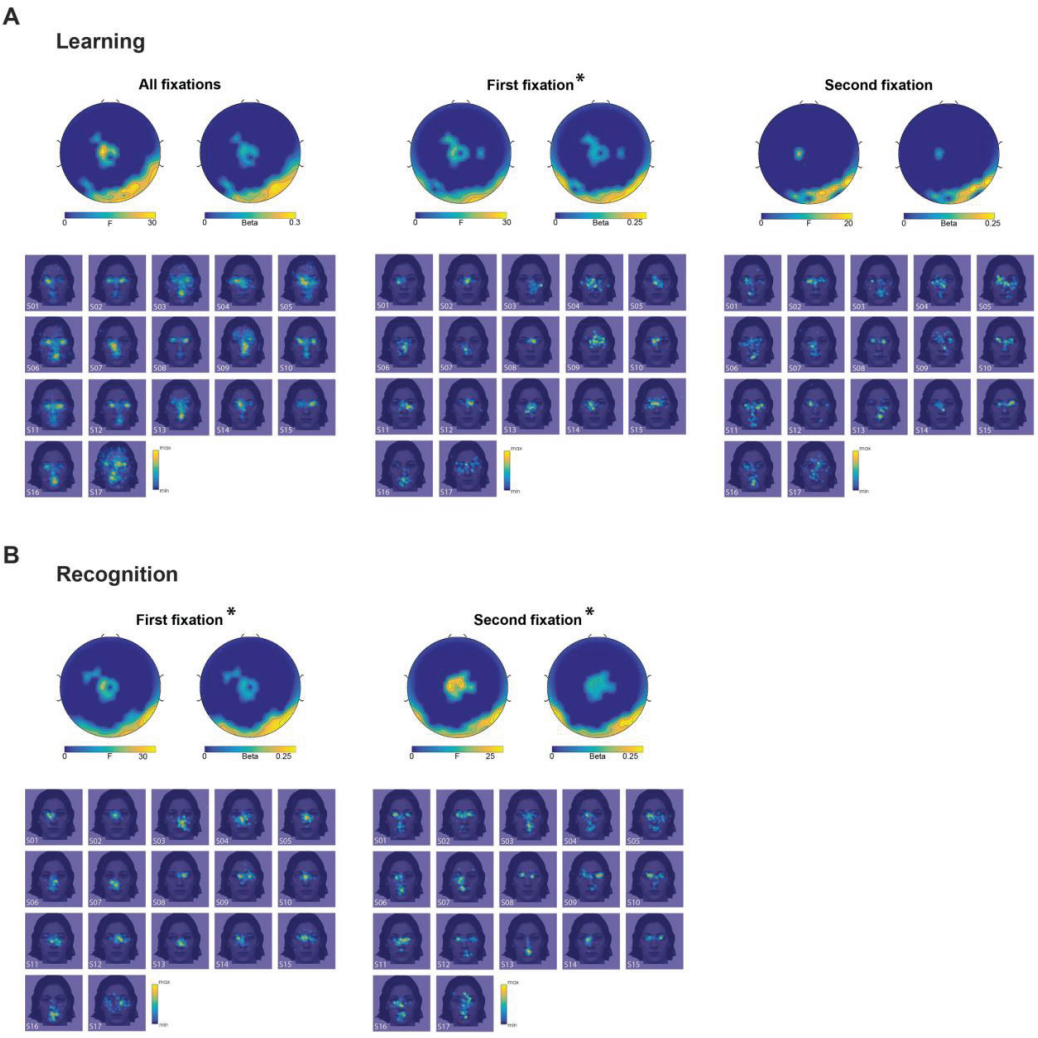

Fig. 6. Results of the analyses performed using the fixation bias computed based on the learning (A) or recognition (B) data. For the learning analyses are reported for all, only the first or second fixation. For the recognition session, analyses are reported for only the first or second fixation. F- and beta-values are reported only electrodes showing a significant ($p < 7.81e\text{-}05$) are shown. Below each topography of the effect are the fixation maps of all observers. * indicates which effect was significant at the simulated threshold.

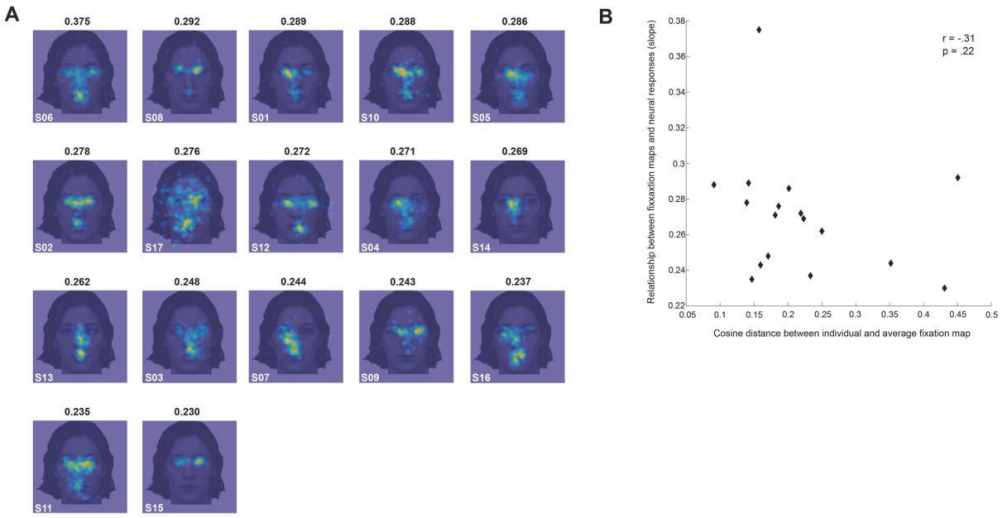

Fig. 7. Fixation maps and strength of the fixation-neural-bias relationship. (A) Observers' fixation maps sorted as a function of the slope of observers' relationship between fixation bias and neural face discrimination response amplitude. The slope is reported for the occipito-temporal electrode showing the strongest effect (i.e., P10). (B) The scatterplot illustrates the lack of correlation between: the cosine distance of individuals' fixation maps from the average fixation map (y-axis) and strength of the relationship between fixation and neural bias (x-axis). Data show there was not a particular fixation bias more likely to correlate with the neural bias. Note that a cosine distance of 0 indicates identical fixation maps

TABLES

Table 1. Number of fixations and fixation maps' similarity between learning and recognition session for each observer.

	Average number of fixations (SD)		Cosine distance between learning and recognition fixation maps		
	Learning	Recognition	All fixations	1st fixation	2nd fixation
S1	13.0 (3.6)	3.4 (1.2)	.19	.12	.11
S2	15.6 (2.0)	5.2 (2.0)	.22	.08	.07
S3	15.4 (3.6)	4.5 (2.7)	.28	.09	.07
S4	10.0 (2.7)	5.7 (3.2)	.23	.07	.21
S5	13.9 (2.2)	6.8 (3.8)	.14	.09	.08
S6	17.7 (1.4)	8.4 (4.4)	.22	.05	.06
S7	11.2 (1.9)	3.6 (2.3)	.16	.20	.14
S8	16.1 (1.6)	4.8 (3.1)	.09	.10	.10
S9	13.9 (3.0)	2.2 (0.9)	.62	.09	.08
S10	14.6 (2.6)	3.4 (1.9)	.32	.16	.18
S11	17.0 (1.8)	6.4 (3.0)	.16	.06	.12
S12	16.8 (1.6)	6.8 (4.7)	.18	.03	.13
S13	13.1 (4.0)	3.0 (0.9)	.32	.11	.15
S14	13.9 (4.1)	2.7 (1.6)	.28	.05	.27
S15	11.7 (2.0)	4.0 (1.7)	.06	.03	.14
S16	10.9 (2.7)	4.7 (2.3)	.23	.08	.17
S17	16.0 (3.0)	7.4 (4.5)	.33	.04	.04

545

Table 2. Results for fixation-dependent regression analyses (for the recognition session).

all fixations			1st fixation			2nd fixation		
	F values	ß-values		F values	ß-values		F values	ß-values
Occipito-temporal cluster			Occipito-temporal cluster			Occipito-temporal cluster		
P10	32.91	.27	P10	33.21	.27	P10	24.48	.24
PO10	28.54	.29	I2	28.90	.26	PO10	23.15	.27
I2	27.82	.25	PO12	25.92	.27	Iz	22.43	.21
PO8	24.99	.26	PO10	25.76	.28	I2	20.05	.22
Iz	24.71	.22	POI2	24.43	.22	I1	17.78	.20
O2	24.23	.21	Iz	23.79	.21	PO8	17.17	.22
PO12	23.90	.26	I1	22.45	.22	PO11	17.08	.20
TP8	21.95	.12	PO11	17.92	.23	PO12	16.82	.22
POI2	20.15	.21	O2	17.32	.18	O2	16.16	.18
I1	19.60	.21	POI1	16.70	.18	POI2	16.02	.19
P8	18.05	.17	Oiz	15.87	.18	POI1	15.94	.17
POI1	17.57	.19	PO8	14.08	.23	P9	13.99	.20
PO11	14.75	.20	P8	13.60	.19	Oiz	13.32	.16
Oiz	14.04	.17	PPO6	13.31	.15			
PO7	13.99	.17						
PPO6	13.75	.14						
P9	13.26	.20						
Centro-parietal cluster			Centro-parietal cluster			Centro-parietal cluster		
C1	33.05	0.14	C1	22.49	0.11	FCC2h	25.49	0.13
C1h	29.70	0.14	FCC1	18.12	0.11	C1	23.89	0.13
FCC2h	26.15	0.13	FCC1h	17.86	0.12	C1h	22.12	0.12
FCC1	24.92	0.14	C1h	16.93	0.10	FCC1	21.69	0.13
FCC1h	23.35	0.14	FCC2h	16.60	0.10	FCC1h	19.77	0.13
C2h	23.12	0.13	CCP1h	15.74	0.10	C2h	19.66	0.12
CCP1h	23.07	0.11	CPz	15.43	0.11	FCz	17.47	0.13
CCPz	19.44	0.13	C2h	15.29	0.10	C4h	16.59	0.09
Cz	17.44	0.12	CCPz	14.39	0.10	CCPz	15.49	0.11
C4	17.00	0.10	FC5h	14.16	0.10	Cz	15.46	0.11
C4h	16.87	0.09	FFC3h	13.80	0.11	FCC2	14.21	0.10
C3h	16.57	0.09				CPz	13.86	0.10
CPz	15.64	0.11				C2	13.85	0.10
FCz	15.42	0.12				CCP1h	13.48	0.08
C2	14.97	0.10				FCC2h	13.37	0.09
Pvalue range: 4.1e-08-3.6e-04			Pvalue range: 3.9e-08-3.5e-04			Pvalue range: 1.1e-06 – 3.5e-04		
Summed F-values		670.9	Summed F-values		474.07	Summed F-values		500.79
Simulated threshold		536.32	Simulated threshold		345.67	Simulated threshold		310.82

546 Reported here are significant (Bonferroni corrected) electrodes for each fixation-dependent analysis
547 (ranked by F-values). For each analysis we report summed F-values and the simulated threshold
548 determined through the random iterations (see Analysis).

549
550

Table 3. Results for fixation-dependent regression analyses (for the learning session).

all fixations			1st fixation			2nd fixation		
	F values	ß-values		F values	ß-values		F values	ß-values
Occipito-temporal cluster			Occipito-temporal cluster			Occipito-temporal cluster		
O2	29.65	0.22	I2	31.97	0.27	O2	20.00	0.19
I2	29.41	0.26	POI2	24.44	0.22	PO10	17.79	0.24
PO8	28.32	0.28	Iz	24.13	0.21	O1	17.69	0.19
PO10	27.82	0.29	PO12	22.02	0.25	P10	17.57	0.22
Iz	26.91	0.22	I1	20.55	0.21	I2	17.23	0.21
P10	23.25	0.23	PO10	18.55	0.26	Oz	17.13	0.15
Oz	22.00	0.18	POI1	18.03	0.19	POI2	15.51	0.19
POI1	21.38	0.20	Oiz	17.85	0.18	PO8	14.60	0.21
PO12	21.37	0.25	PO11	17.32	0.22	POI1	14.22	0.17
POI2	19.82	0.21	P10	16.41	0.23			
P9	18.22	0.10	O2	16.21	0.17			
Oiz	17.77	0.18	Oz	15.17	0.16			
I1	17.02	0.20	PO7	13.92	0.16			
TP8	15.78	0.10	P9	13.80	0.20			
P8	15.33	0.16						
PPO6	15.16	0.15						
PO7	13.36	0.16						
Centro-parietal cluster			Centro-parietal cluster			Centro-parietal cluster		
C1	26.53	0.13	C1	20.22	0.11	C1	18.01	0.11
FCC1	23.18	0.13	FFC3h	19.63	0.13			
FCC5h	22.21	0.12	FCC1h	18.24	0.12			
FCC1h	20.12	0.13	FCC1	17.06	0.11			
C2h	19.25	0.12	CCP1h	15.72	0.09			
FCC2h	17.69	0.11	C2h	15.03	0.10			
CPz	14.85	0.11	FCC2h	14.90	0.10			
Cz	14.30	0.11	CCPz	14.21	0.10			
FFC3h	13.67	0.11	C1h	14.17	0.10			
			FFC1	14.01	0.10			
			C4	13.77	0.08			
Pvalue range: 1.8e-07 - 3.4e-04			Pvalue range: 6.6e-08 - 2.8e-04			Pvalue range: 1.4e-05 - 2.2e-04		
Summed F-values		534.39	Summed F-values		447.33	Summed F-values		169.73
Simulated threshold		534.96	Simulation threshold		315.06	Simulated threshold		447.35

551 Reported here are significant (Bonferroni corrected) electrodes for each fixation-dependent analysis
552 (ranked by F-values). For each analysis we report summed F-values and the simulated threshold
553 determined through the random iterations (see Analysis).
554
555

556